



Delineation of podiform-type chromite mineralization using geochemical mineralization prospectivity index and staged factor analysis in Balvard area (SE Iran)

P. Afzal^{1*}, M. Yousefi², M. Mirzaei¹, E. Ghadiri-Sufi³, S. Ghasemzadeh⁴ and L. Daneshvar Saein⁵

1. Department of Petroleum and Mining Engineering, South Tehran Branch, Islamic Azad University, Tehran, Iran

2. Faculty of Engineering, Malayer University, Malayer, Iran

3. Department of Mining Engineering, Kashan University, Kashan, Iran

4. Department of Mining and Metallurgy Engineering, Amirkabir University of technology (Tehran Polytechnic), Tehran, Iran

5. Department of Geology, Payame Noor University, Tehran, Iran

Received 19 February 2019; received in revised form 27 May 2019; accepted 9 June 2019

Keywords

Geochemical
Mineralization
Prospectivity Index
Staged Factor Analysis
Continuous Weighting
Fuzzy Logic
Podiform-Type Chromite

Abstract

The aim of this work was to delineate the prospects of podiform-type chromite by staged factor analysis and geochemical mineralization prospectivity index in Balvard area, SE Iran. The stream sediment data and fault density were used as the exploration features for prospectivity modeling in the studied area. In this regard, two continuous fuzzified evidence layers were generated and integrated using fuzzy operator. Then fractal modeling was used for defuzzification of the prospectivity model obtained. Furthermore, the prediction-area plot was used for evaluation of the predictive ability of the generated target areas. The results obtained showed that using the prospectivity model, 82% of mineral occurrences was predicted in 18% of the studied area. In addition, the target areas were correlated with the geological particulars including ultrabasic and serpentinization rocks, the host rocks of the podiform-type chromite deposit type.

1. Introduction

Mineral potential mapping (MPM) is a multi-step procedure of constructing evidential maps, combining them, and finally, ranking the generated target areas for further exploration. The knowledge and data-driven methods are two types of techniques used to assign the evidential weights and combine different evidential maps for MPM [1, 2].

Integration of the stream sediment geochemical data with other types of mineral exploration data in knowledge-driven MPM is a challenging issue that requires careful analysis of multi-element geochemical anomalies as an evidence of the presence of the deposit-type sought [2, 3]. In this regard, factor analysis (FA), as one of the multivariate analysis methods, has been widely used for explanation of the geochemical data [4-8]. The principal purpose of FA is to define the variations in a multivariate dataset by a few

factors as much as possible and to detect the hidden multivariate data structures [9, 10]. To improve the results of multi-elemental analyses of geochemical data, Yousefi *et al.* (2012, 2014) [3, 11] proposed staged factor analysis (SFA), in which geochemical noses and non-indicator elements were recognized and excluded from the analyses to obtain significant multi-element signatures of the deposit type sought.

In addition, Yousefi *et al.* (2012, 2014) [3, 11] proposed to transform the values of the factor scores obtained into a logistic space for calculating a geochemical mineralization prospectivity index (GMPI). GMPI is a transformed value of multi-element geochemical signatures into the [0, 1] range. Thus a distribution map of GMPI of geochemical signature can be used as a fuzzy evidence layer for MPM [3, 11-15].

Exploration of podiform-type chromite deposits is important in Iran based on the geological and economical parameters. There are many small podiform deposits in different ophiolitic zones [16, 17]. Geochemical signatures for this mineralization type are difficult for interpretation and require accurate detection and recognition [16-18]. Roshanravan *et al.* (2018a,b and 2019) recognized geochemical signatures of podiform-type chromite deposits in the North of Iran (Sabzevar ophiolite belt) by a logistic-based method [19-21]. The results of these studies showed that a neuro-fuzzy model generated with continuously weighted spatial evidence values was superior to that of the neuro-fuzzy model generated with discretely weighted exploration evidence data [19-21]. The purpose of this work was to generate target areas for further exploration of podiform-type chromite mineralization in Balvard area (SE Iran) using the geochemical and geological datasets. For this, we interpreted geochemical multi-element data to obtain a significant multi-element geochemical signature of the deposit type sought. In this regard, we applied SFA and GMPI to generate a continuous weighted geochemical evidence layer [13-15]. Based on the deposit model, we used a map of fault density (FD) in the studied area as another exploration feature of the deposit type sought. For generating a weighted evidence layer of FD, we applied the continuous weighting approach proposed by Yousefi *et al.* (2014) [11] and Yousefi and Carranza (2014, 2015a, 2015b) [13-15]. Then since either of the generated evidence layers were continuous and weighted in the [0, 1] range, we used fuzzy operator to integrate the evidence layers and to generate the target areas for further exploration.

In this work, SFA and GMPI were applied for generation of an MPM for podiform-type chromite mineralization. Classification of geochemical anomalies based on the results obtained by SFA and GMPI can differ depending on the variety of elemental associations and dispersion patterns of geochemical element caused by geological settings of the studied area. For defuzzification of the prospectivity model and for evaluation of the generated target areas, we used fractal analysis [e.g. 16] and prediction-area

(P-A) plot [13, 15] using location of the known mineral occurrences in the studied area.

2. Geological setting of Balvard area

The studied area is located on the 1:100000 geological quadrangle map of Balvard in the Kerman Province, SE Iran. The area is located on the Nain-Baft Ophiolitic belt in the structural-metamorphic Sanandaj-Sirjan zone of Iran (SSZ: Figure 1: [22]). The SSZ trends northwestward in the western Iran on the Precambrian to Paleozoic basement, and exposes abundant Late Jurassic to Upper Cretaceous I-type granitoids and calc-alkaline volcanic rocks [23].

The Nain-Baft ophiolitic belt (Central Iran) extends in a NW-SE direction parallel to the Sanandaj-Sirjan Zone (Figure 1: [22]). The outcropping rocks in this belt are slices of harzburgites, small bodies of gabbros, and dike swarm complexes, accompanied by various volcanic rocks with composition of basaltic-andesitic lava flows and breccias to dacites and rhyolites [22-24].

The ophiolite units are located in the NE part of the area with a composition of ultramafic and mafic rocks (such as diabase and serpentinite), capped by pelagic sediments resting directly on the ophiolite (Figure 1: [22]). The Paleozoic units consisting of ortho-gneiss, muscovite, quartz, microcline, and albite occurred in the northern part of the studied area. Limestones and biotite-chlorite-amphibole schist units outcrop in the northern and NE parts of the area (Figure 1: [25, 26]).

There are several alterations consisting of chloritization, epidotization, and carbonization. Eocene volcanics include trachyandesite and trachybasalt within the pyroclastic rocks occurring in the NE part of the area (Figure 1). Based on the rock types and the geological indicator, the studied area has a good potential for prospecting chromite and titanomagnetite mineralization [22]. However, in this work, the purpose is to generate targets for chromite mineralization. The Balvard-Baft ophiolite is in fault or unconformable contact with Middle to Late Eocene sedimentary-volcanic sequences related to the Urumieh–Dokhtar magmatic arc [27].

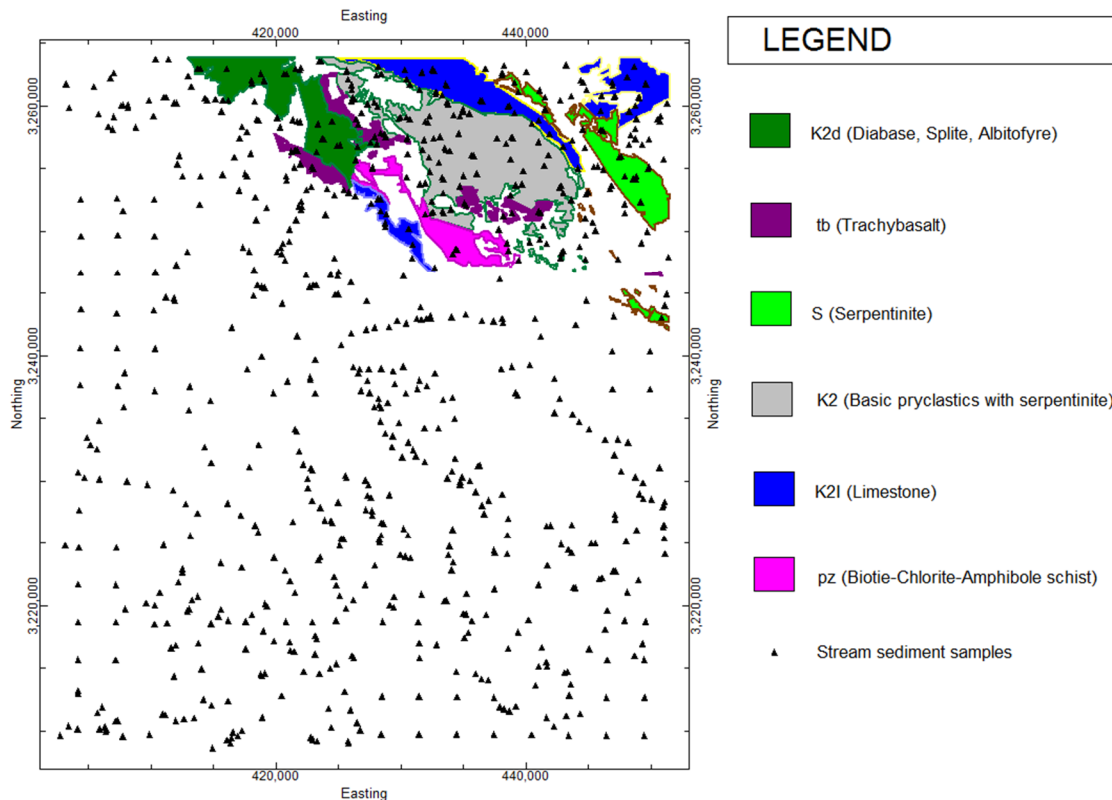


Figure 1. Simplified Geological map of Balvard 1:100,000 sheet within sample locations the Nain-Baft ophiolites in the structural-metamorphic Sanandaj - Sirjan zone.

3. Methods

3.1. Staged factor analysis to recognize clean factor(s)

Analysis of significant anomalies in geochemical landscapes based on the stream sediment geochemical data is important for creating and integrating layers of geochemical evidence in MPM for the deposit-type sought [3, 28]. In this regard, we used multi-element (Cr, Ni, Co, Fe, Mn, Ti, Mg, V, and K) concentration data from 168 samples of -80 mesh (<177 μm) fraction of stream sediments, collected, analyzed, and prepared by the Geological Survey of Iran (GSI). To determine a multi-element anomalous signature of the deposit-type sought, we performed SFA [11]. SFA is a multivariate analysis for well-organized extraction of significant multi-element anomalous signature. In this method, to recognize multi-element associations in a geochemical dataset, non-indicator (noisy) elements are progressively delineated and excluded from the analysis until a satisfactory significant multi-element signature is obtained [11]. Prior to performing SFA, the isometric logratio (ilr) transformation [29, 30] was applied on the multi-element geochemical data to address the closure problem inherent in the compositional data [29-31]. Open and raw data correlation matrix is depicted in Figure 2. The

data was back-transformed according to the following formula based on arithmetic mean as \bar{z} [30]:

$$\bar{x} = \frac{\exp(\sqrt{2z})}{\exp(\sqrt{2z}) + 1} \quad (1)$$

Moreover, classical principle component analysis (PCA) with varimax rotation [32] was used for extracting the common factors, and we considered only factors with eigenvalues of >1 for interpretation. Additionally, we used 0.6 as the threshold value for loadings in FA to extract significant multi-element geochemical signature of the deposit-type sought. A threshold value for minimum loading criterion for elemental variables should be selected between 0.3 and 0.6 in order to reduce the errors of the calculation of the scores in factor analysis [e.g. 3, 4, 11, 33]. As a result of SFA, which is depicted in Table 1, two multi-element associations (i.e. factors) were recognized consisting of F1 (Fe-Mn-Ti-V) and F2 (Cr-Ni-Co-Mg). K is a noisy element based on the result of first stage FA in Table 1. Thus it must be excluded from the dataset in the second stage FA (Table 1). According to the results of SFA, F2 was selected as multi-element signature of the deposit type sought, podiform type of chromite deposit.

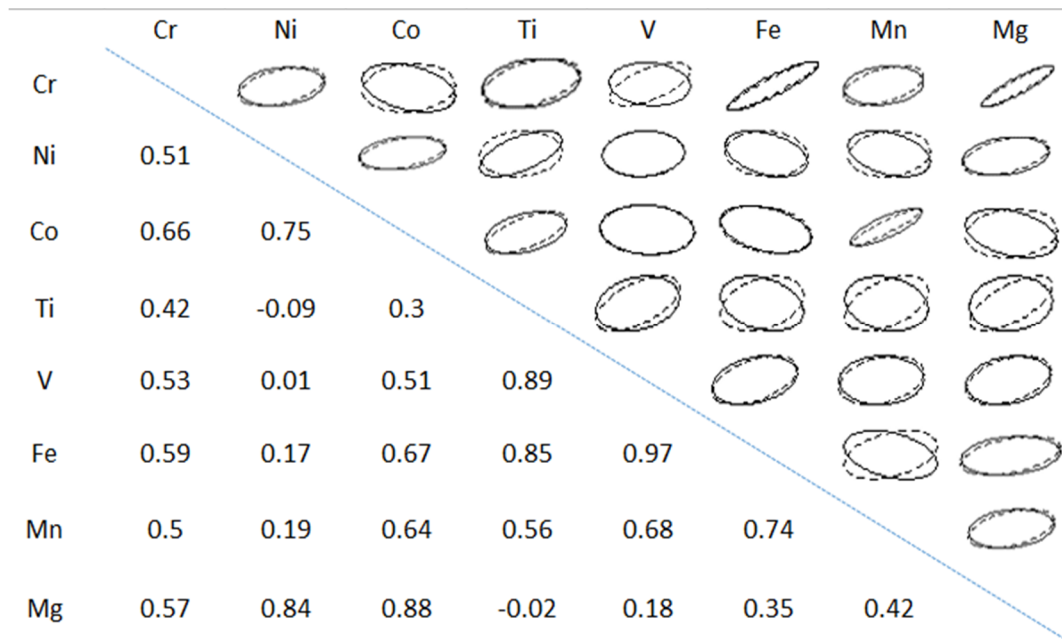


Figure 2. Open and raw data correlation matrix.

Table 1. Rotated component matrix of the first and second steps of factor analysis. Loadings in bold represent the selected elements based on a threshold of 0.6 (the absolute threshold value).

Element	First step		Second step		
	F1	F2	F1	F2	
Cr	.501	.684	Cr	.490	.677
Ni	.063	.930	Ni	.028	.943
Co	.547	.780	Co	.514	.811
Fe	.892	.392	Fe	.875	.429
Mn	.774	.374	Mn	.758	.405
Ti	.941	-.081	Ti	.945	-.055
Mg	.207	.903	Mg	.166	.931
V	.949	.219	V	.943	.245
K	-.053	-.427			

3.2. Generation of GMPI map

The derived sample factor scores (FSs) depicting significant multi-element signatures of the deposit-type sought (here F2) usually lie outside the [0, 1] range. Therefore, a logistic sigmoid function was used to calculate a GMPI, a derived geochemical multi-element signature of the deposit-type sought in a weight space, to create fuzzy geochemical evidence maps, as follows:

$$GMPI = \frac{e^{FS}}{1 + e^{FS}} \quad (2)$$

where FS is the factor score of each sample per indicator component achieved by factor analysis. GMPI is a fuzzy weight assigned to stream sediment samples to represent their relative

importance for prospecting the mineral deposit-type sought. Moreover, using GMPI, the evidential scores of stream sediment samples are calculated continuously based on the FSs of samples [3, 13].

In this work, the FS values of indicator factor, F(Cr-Ni-Co-Mg), were unbounded, so we used Eq. (1) to transform the FS values to logistic space. Yousefi *et al.* (2012; 2014) [3, 13] have demonstrated that a GMPI map is an enhanced weighted geochemical evidence layer compared to a geochemical evidence layer generated based on the results of ordinary FA. The GMPI distribution map of podiform type chromite deposit (*GMPI Chromite*) is depicted in Figure 3.

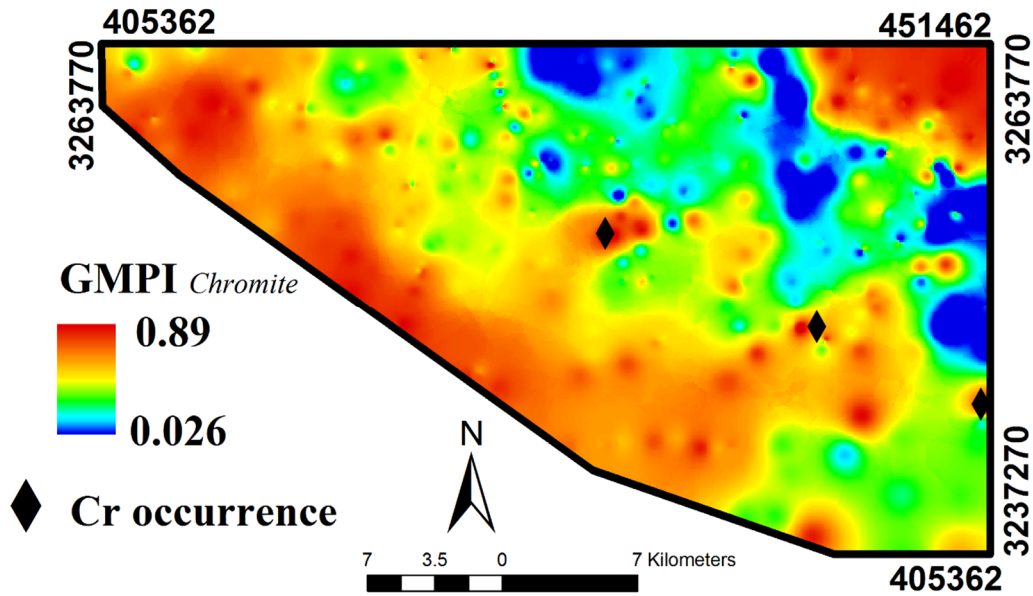


Figure 3. Distribution map of $GMPI_{Chromite}$

3.3. Generation of structure evidential map

Structural investigations have recognized the important role of enhanced rock permeability in forming mineral deposits [34]. The presence of structural discontinuities is generally considered to be a major criterion for the presence of deposits. Faults facilitate the passage of magmas and the circulation of hydrothermal fluids [cf. 35-37]. Faults/fractures are common loci of many types of mineral deposits, and thus the presence of such geological features indicates the enhanced structural permeability of rocks in the sub-surface [2]. It is generally accepted that fault zones act as major channel ways for

deeply-sourced melts as well as hydrothermal fluids [37].

Fault investigations have been used to study chromite mineralization in the literature [20]. Thus areas with high FD represent favorability for podiform-type chromite deposits. In this work, we used FD as an evidence layer to prospect the deposit-type sought. To generate the FD map, the total length of faults per pixel of the studied area was calculated. Then because the FD values were unbounded, for generating a weighted evidence layer, we applied Eq. (3) from Yousefi *et al.* (2014) [11], a logistic function, for transforming the FD values to weight space, fuzzy space (Figure 4).

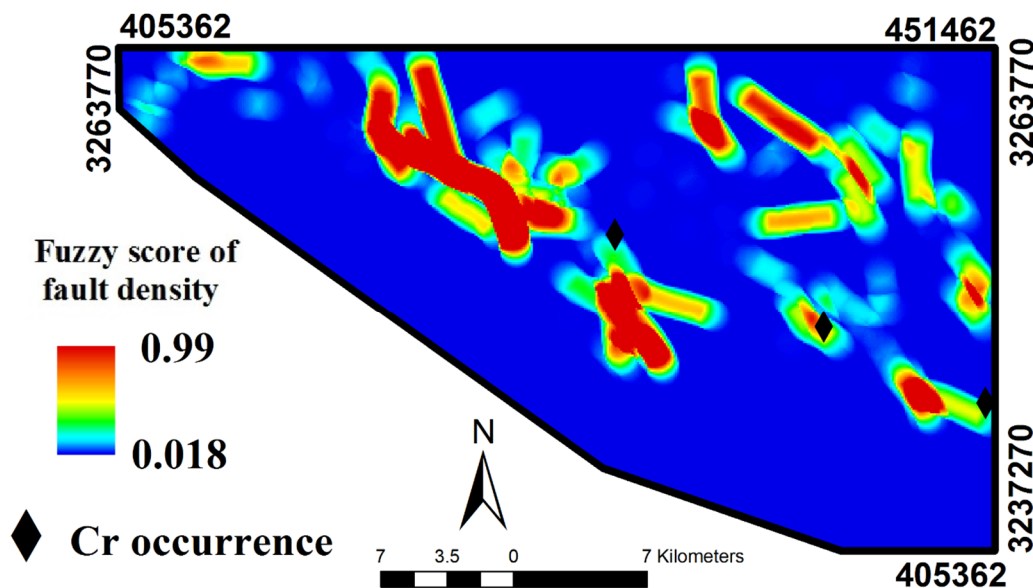


Figure 4. Fuzzy score of fault density.

3.4. Integration of weighted evidence layers

In fuzzy MPM, the fuzzy evidence maps (Figures 3 and 4) are combined to obtain a map of fuzzy prospectivity values for delineating the target areas for further exploration of the mineral deposit-type sought [2, 3]. Fuzzy evidence maps are integrated using suitable fuzzy operators [38]. In this regard, any of the existing fuzzy operators can be used considering the mineralization type sought and the purpose of the integration. We used the fuzzy gamma operator to integrate the weighted evidential maps (Figure 5) because it involved both the fuzzy algebraic sum and fuzzy algebraic product operators in a scheme. The output of the fuzzy algebraic product is less than or equal to the lowest fuzzy score at every location in the input fuzzy evidence maps. Thus the fuzzy algebraic product has a ‘decreaseive’ effect, meaning that the presence of very low but non-zero fuzzy scores tends to deflate or underestimate the overall support for the proposition, and so it is appropriate in combining complementary sets of evidence. The output of the fuzzy algebraic sum is greater than or equal to the highest fuzzy score at every location in the input fuzzy evidence maps. Thus the fuzzy

algebraic sum has an ‘increaseive’ effect, meaning that the presence of very high fuzzy scores (but not equal to 1) tends to inflate or overestimate the overall support for the proposition, and so it is appropriate in combining supplementary sets of evidence. Considering that the target areas for prospecting podiform chromite deposits must exhibit the presence of supplementary evidential features representing interactions of conditions favorable for mineral deposit formation, such areas should have high prospectivity values. Consequently, using the fuzzy algebraic sum to model the ‘increaseive’ effect of supplementary sets of evidence is more (but not totally) suitable than using the fuzzy algebraic product to model the ‘decreaseive’ effect of supplementary sets of evidence. To achieve this in a single operation, we used the fuzzy gamma operator with a high value of gamma, which was equal to 0.9.

The results obtained by the map of fuzzy prospectivity score reveal that the main prospects for podiform chromite deposits with a NW-SE trend situated in the central parts of the area (Figure 5). These prospects were validated by the chromite occurrences in the Balvard area, as depicted in Figure 5.

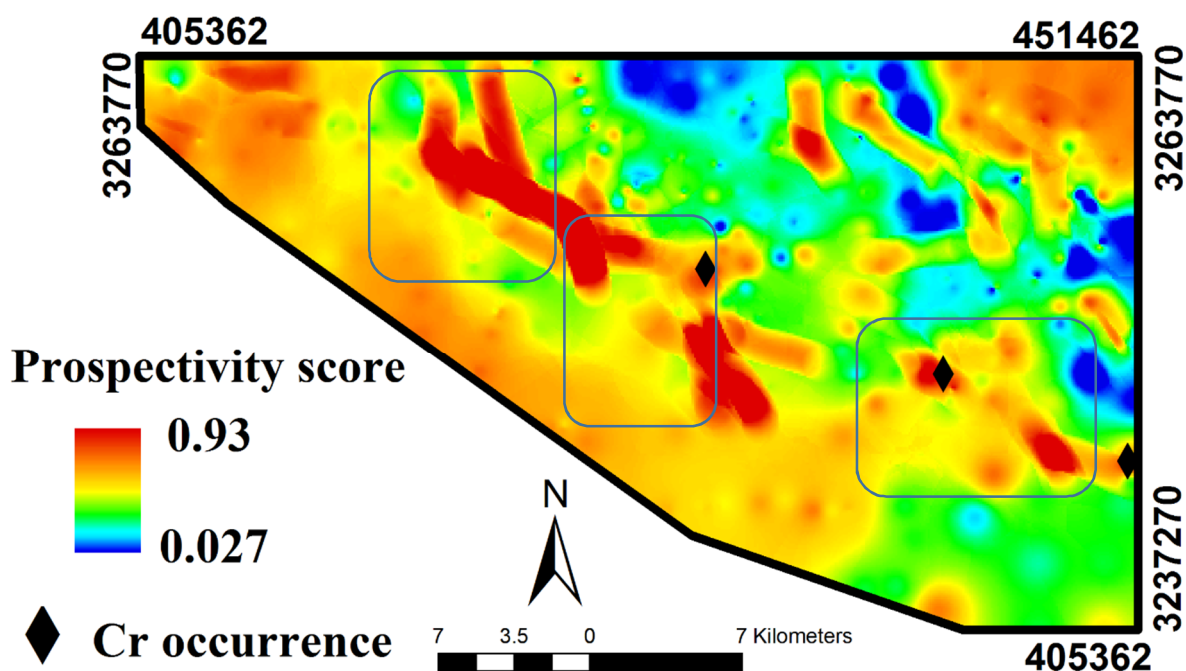


Figure 5. Prospectivity map of chromite in the studied area (selected areas are shown by rectangles).

3.5. Evaluation of the prospectivity map

3.5.1. Using P-A plot

After generation of prospectivity models in a studied area, locations of known mineral deposits of the type sought in the area or field observations can be used as an empirical test to evaluate the

results and to obtain measures of success [e.g. 1, 2, 39-43]. In this work, the locations of known podiform chromite occurrences were used in a P-A plot [13-15] to evaluate the model. For this, the prospectivity values were classified utilizing fractal [43] because as Yousefi and Carranza

(2014; 2015b) [13, 15] illustrated, prospectivity models, a combination of geological features with fractal dimensions [e.g. 2, 44-47] have fractal dimensions as well. In this work, the concentration–area (C–A) model proposed by Cheng *et al.* (1994) [16] was utilized to determine thresholds for classifying the prospectivity values in the fuzzy prospectivity model. Based on P-A the log-log plot (Figure 6), five classes of prospectivity scores are delineated in this area (Figure 6). Based on the P-A log-log plot (Figure 6), there is a multi-fractal nature for chromite prospectivity in this area, which reveals that main chromite prospects commences from prospectivity values higher than 0.57. There are three chromite occurrences that are correlated to the classified prospectivity model of podiform chromite, as depicted in Figure 7. These occurrences were located in the high prospectivity values in the model. After generation of a classified map of prospectivity, the P-A plot [13, 15] was used to quantify the ability of the prospectivity model in prediction of mineral occurrences (Figure 8).

The intersection point of the two curves consisting of prediction rate of known mineral occurrences corresponding to prospectivity classes and the percentage of occupied areas corresponding to the prospectivity classes is a criterion to evaluate the fuzzy prospectivity model (Figure 5) [13, 14]. This is because if an intersection point appears in a higher place in the P–A plot, it depicts a smaller

area containing a larger number of mineral deposits. Thus it is “easier” to find undiscovered deposits type sought in such a smaller area [13, 14]. The intersection point of the P–A plot for fuzzy prospectivity model (Figure 7) shows 82% of mineral occurrences predicted only in 18% of the studied area. Mihalasky and Bonham-Carter (2001) [48] used the prediction rate of mineral occurrences of each class of evidential layers divided by their corresponding occupied area, termed as normalized density, to recognize positive and negative association of mineral occurrences by classes of evidential values. Mihalasky and Bonham-Carter (2001) [48, 49] mentioned that the normalized density >1 was a proper predictor of the deposit type sought. Yousefi and Carranza (2015b) [15] used the parameters extracted from an intersection point of the P-A plot of an evidence layer (or a prospectivity map) for evaluating individual evidence layers (or different prospectivity models). For this, the prediction rate and occupied area are extracted from intersection point of the P-A plot, then the value of prediction rate is divided by the value of occupied area to calculate normalized density of the prospectivity model. For prospectivity model in this paper, the value of normalized density is 4.55 (82/18). Thus as Mihalasky and Bonham-Carter (2001) [48] mentioned the model as a predictor of the ore deposit-type.

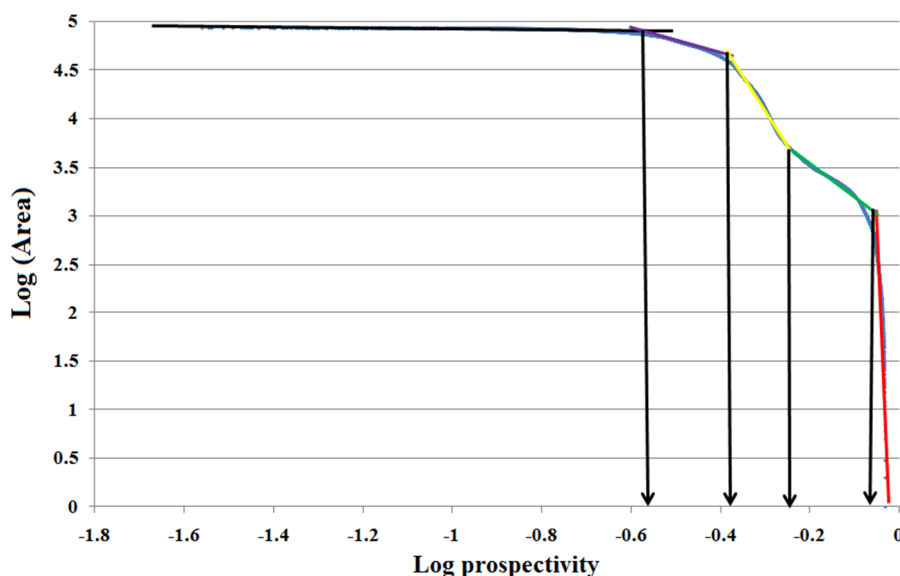


Figure 6. Log-log plot of fuzzy prospectivity values in the Balvard area.

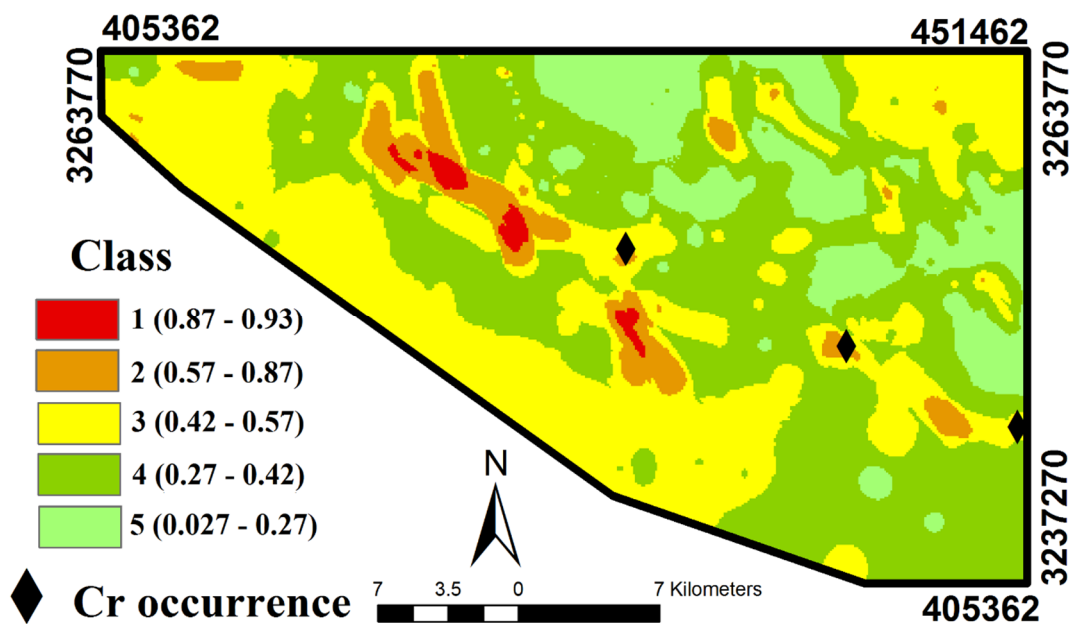


Figure 7. Classified map of chromite prospectivity model using C-A fractal model.

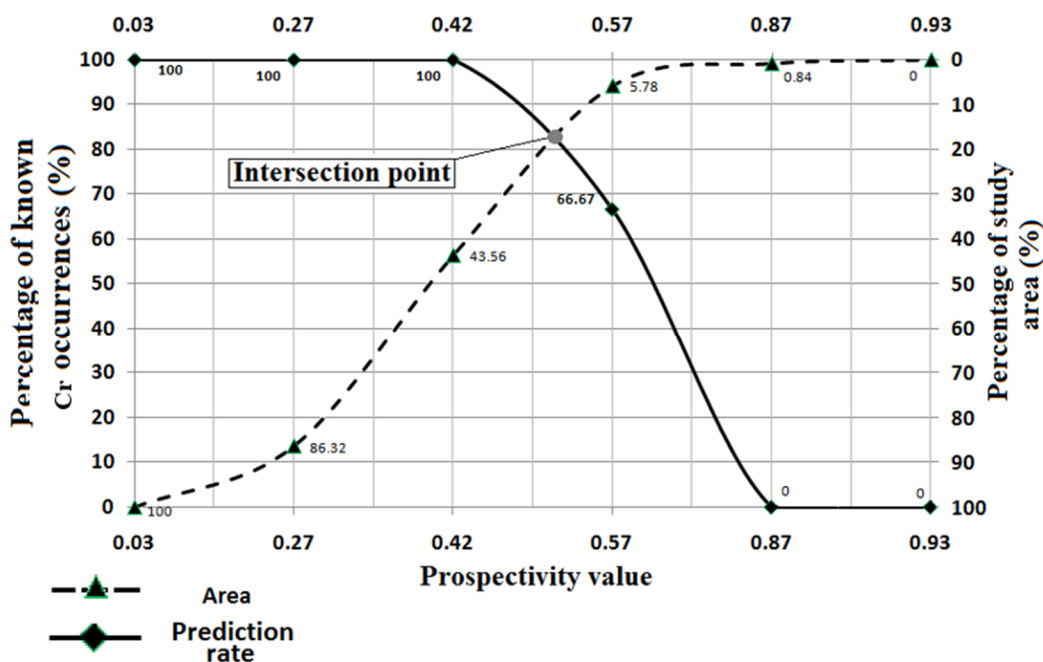


Figure 8. P-A plot for fuzzy prospectivity model in Figure 4.

3.5.2. Mineralization and field observations

In this paper, considering the prospectivity map, Figure 6, the areas with high values of prospectivity were selected for field observation (Figure 5). Fieldwork can be conducted in the delimited target areas to evaluate/validate MPM results because MPM aims to delimit target areas for further exploration of this deposit-type. This operation showed that the areas with high values of $GMPI_{Chromite}$ are correlated with chromite occurrences in the studied area (Figure 8). Furthermore, three podiform chromite

occurrences have a good correlation with determined areas by GMPI and the staged factor analysis. Thus the area with high $GMPI_{Chromite}$ values can be selected as the target area for further exploration of undiscovered podiform chromite deposits in the studied area.

F1 (Fe-Mn-Ti-V) and F2 (Cr-Ni-Co-Mg) can be represented titanomagnetite and chromite mineralization, respectively. Moreover, the existing serpentinization and high fault density values in the area have a positive influence with chromite ore mineralization, especially in the NE

and northern parts of the studied area (Figures 1, 3, and 4).

4. Conclusions

The results of this work show that GMPI and SFA can be used for a better interpretation for generation of an MPM. The target areas obtained by the methodology have a spatial association with known podiform chromite occurrences. Furthermore, combination among GMPI, fractal modelling, and staged factor analysis is a useful method for prospecting of metallic ore deposits, especially podiform chromite. The staged factor analysis can be effectively utilized to remove pseudo-anomalies and recognize major anomalies in the Balvard area. Based on the results obtained in this work, there are chromite ore prospects in the NE and northern parts of the Balvard area. In addition, field observations show geological features including ultrabasic rocks and serpentization, which represent evidence of podiform chromite mineralization in the area. Moreover, the Cr occurrences are correlated with this result, which validate the method for future challenges.

Acknowledgments

The authors would like to thank the editors and reviewers of this paper for their comments and valuable remarks.

References

[1]. Bonham-Carter, G.F. (1994). Geographic Information Systems for Geoscientists, Volume 13: Modelling with GIS (Computer Methods in the Geosciences).

[2]. Carranza, E.J.M. (2008). Geochemical anomaly and mineral prospectivity mapping in GIS (Vol. 11). Elsevier.

[3]. Yousefi, M., Kamkar-Rouhani, A. and Carranza, E.J.M. (2012). Geochemical mineralization probability index (GMPI): a new approach to generate enhanced stream sediment geochemical evidential map for increasing probability of success in mineral potential mapping. *Journal of Geochemical Exploration*. 115: 24-35.

[4]. Bovec, Z. (1996). Evaluation of the concentrations of trace elements in stream sediments by factor and cluster analysis and the sequential extraction procedure. *Science of the Total Environment*. 177 (1-3): 237-250.

[5]. Van Helvoort, P.J., Filzmoser, P. and van Gaans, P.F. (2005). Sequential Factor Analysis as a new approach to multivariate analysis of heterogeneous geochemical datasets: An application to a bulk

chemical characterization of fluvial deposits (Rhine-Meuse delta, The Netherlands). *Applied geochemistry*. 20 (12): 2233-2251.

[6]. Reimann, C., Filzmoser, P. and Garrett, R.G. (2002). Factor analysis applied to regional geochemical data: problems and possibilities. *Applied geochemistry*. 17 (3): 185-206.

[7]. Grunsky, E.C., Drew, L.J. and Sutphin, D.M. (2009). Process recognition in multi-element soil and stream-sediment geochemical data. *Applied geochemistry*. 24 (8): 1602-1616.

[8]. Sun, X., Deng, J., Gong, Q., Wang, Q., Yang, L. and Zhao, Z. (2009). Kohonen neural network and factor analysis based approach to geochemical data pattern recognition. *Journal of Geochemical Exploration*. 103 (1): 6-16.

[9]. Krumbein, W.C. and Graybill, F.A. (1965). An introduction to statistical models in geology. McGraw-Hill.

[10]. Tripathi, V.S. (1979). Factor analysis in geochemical exploration. *Journal of Geochemical Exploration*. 11 (3): 263-275.

[11]. Yousefi, M., Kamkar-Rouhani, A. and Carranza, E.J.M. (2014). Application of staged factor analysis and logistic function to create a fuzzy stream sediment geochemical evidence layer for mineral prospectivity mapping. *Geochemistry: Exploration, Environment, Analysis*. 14 (1): 45-58.

[12]. Yousefi, M., Carranza, E.J.M. and Kamkar-Rouhani, A. (2013). Weighted drainage catchment basin mapping of stream sediment geochemical anomalies for mineral potential mapping. *Journal of Geochemical Exploration*. 128: 88-96.

[13]. Yousefi, M. and Carranza, E.J.M. (2016). Data-driven index overlay and Boolean logic mineral prospectivity modeling in greenfields exploration. *Natural Resources Research*. 25 (1): 3-18.

[14]. Yousefi, M. and Carranza, E.J.M. (2015). Fuzzification of continuous-value spatial evidence for mineral prospectivity mapping. *Computers & Geosciences*. 74: 97-109.

[15]. Mirzaei, M., Afzal, P., Adib, A., Kahalajmasoumi, M. and Zia Zarifi, A. (2014). Prospection of Iron and Manganese Using Index Overlay and Fuzzy Logic Methods in Balvard 1:100,000 Sheet, SE Iran. *Iranian Journal of Earth Sciences*. 6: 1-11.

[16]. Mosier, D.L., Singer, D.A., Moring, B.C. and Galloway, J.P. (2012). Podiform chromite deposits database and grade and tonnage models. US Geological Survey Scientific Investigations Report, 5157, 45.

[17]. Tarrach, J., Abedpour, G., Strauss, K., Schirmer, T. and Mengel, K. (2015). Mineralogical and

geochemical investigations of chromite ores from ophiolite complexes of SE Iran in terms of chrome spinel composition. *Iranian Journal of Earth Sciences*. 7: 114-123.

[18]. Yigit, O. (2009). Mineral deposits of Turkey in relation to Tethyan metallogeny: implications for future mineral exploration. *Economic Geology*. 104 (1): 19-51.

[19]. Roshanravan, B., Agajani, H., Yousefi, M. and Kreuzer, O. (2018a) Generation of a Geochemical Model to Prospect Podiform Chromite Deposits in North of Iran. 80th EAGE Conference and Exhibition 2018, DOI: 10.3997/2214-4609.201800909.

[20]. Roshanravan, B., Agajani, H., Yousefi, M. and Kreuzer, O. (2018b) An Improved Prediction-Area Plot for Prospectivity Analysis of Mineral Deposits. *Natural Resources Research*. doi.org/10.1007/s11053-018-9439-7.

[21]. Roshanravan, B., Agajani, H., Yousefi, M. and Kreuzer, O. (2019) Particle Swarm Optimization Algorithm for Neuro-Fuzzy Prospectivity Analysis Using Continuously Weighted Spatial Exploration Data. *Natural Resources Research*. 28: 309-325.

[22]. Arfania, R. (2018). Role of supra-subduction zone ophiolites in the tectonic evolution of the southeastern Zagros Orogenic Belt, Iran. *Iranian Journal of Earth Sciences*. 10: 31-38.

[23]. Moghadam, H.S., Stern, R.J., Chiaradia, M. and Rahgoshay, M. (2013). Geochemistry and tectonic evolution of the Late Cretaceous Gogher-Baft ophiolite, central Iran. *Lithos*. 168: 33-47.

[24]. Tarrah, J. (2016). Normative calculation of mineral composition in Cr ores of the ophiolite complexes from SE Iran. *Iranian Journal of Earth Sciences*. 8 (1): 36-44.

[25]. Ghazi, J.M., Moazzen, M., Rahgoshay, M. and Moghadam, H.S. (2012). Geochemical characteristics of basaltic rocks from the Nain ophiolite (Central Iran); constraints on mantle wedge source evolution in an oceanic back arc basin and a geodynamical model. *Tectonophysics*. 574: 92-104.

[26]. Srdic, A., Dimitrijevic, M.N., Cvetic, S. and Dimitrijevic, M.D. (1972). Geological Map of Baft. 1/100000 Series, Sheet 7348. Geological survey of Iran.

[27]. Moghadam, H.S. and Stern, R.J. (2015). Ophiolites of Iran: Keys to understanding the tectonic evolution of SW Asia:(II) Mesozoic ophiolites. *Journal of Asian Earth Sciences*. 100: 31-59.

[28]. Carranza, E.J.M. (2010). Mapping of anomalies in continuous and discrete fields of stream sediment geochemical landscapes. *Geochemistry: Exploration, Environment, Analysis*. 10 (2): 171-187.

[29]. Egozcue, J.J., Pawlowsky-Glahn, V., Mateu-Figueras, G. and Barcelo-Vidal, C. (2003). Isometric logratio transformations for compositional data analysis. *Mathematical Geology*. 35 (3): 279-300.

[30]. Filzmoser, P., Hron, K. and Reimann, C. (2009). Univariate statistical analysis of environmental (compositional) data: problems and possibilities. *Science of the Total Environment*. 407 (23): 6100-6108.

[31]. Hoseinzade, Z. and Mokhtari, A.R. (2017) A comparison study on detection of key geochemical variables and factors through three different types of factor analysis. *Journal of African Earth Sciences*. 134: 557-563.

[32]. Carranza, E.J.M. (2011). Analysis and mapping of geochemical anomalies using logratio-transformed stream sediment data with censored values. *Journal of Geochemical Exploration*. 110 (2): 167-185.

[33]. Afzal, P., Eskandarnejad Tehrani, M., Ghaderi, M. and Hosseini, M.R. (2016). Delineation of supergene enrichment, hypogene and oxidation zones utilizing staged factor analysis and fractal modeling in Takht-e-Gonbad porphyry deposit, SE Iran. *Journal of Geochemical Exploration*. 161: 119-127.

[34]. Treiblmaier, H. and Filzmoser, P. (2010). Exploratory factor analysis revisited: How robust methods support the detection of hidden multivariate data structures in IS research. *Information & management*. 47 (4): 197-207.

[35]. Mickelthwaite, S., Sheldon, H.A. and Baker, T. (2010). Active fault and shear processes and their implications for mineral deposit formation and discovery. *Journal of Structural Geology*. 32 (2): 151-165.

[36]. Cox, D.P. and Singer, D.A. (1986). Mineral deposit models (Vol. 1693). Bulletin: US Government Printing Office.

[37]. Sillitoe, R.H. (1997). Characteristics and controls of the largest porphyry copper-gold and epithermal gold deposits in the circum-Pacific region. *Australian Journal of Earth Sciences*. 44 (3): 373-388.

[38]. Pirajno, F. (2008). Hydrothermal processes and mineral systems. Springer Science & Business Media.

[39]. An, P., Moon, W.M. and Rencz, A. (1991). Application of fuzzy set theory for integration of geological, geophysical and remote sensing data. *Canadian Journal of Exploration Geophysics*. 27 (1): 1-11.

[40]. Agterberg, F.P. and Bonham-Carter, G.F. (2005). Measuring the performance of mineral-potential maps. *Natural Resources Research*. 14 (1): 1-17.

[41]. Porwal, A., Carranza, E.J.M. and Hale, M. (2004). A hybrid neuro-fuzzy model for mineral

potential mapping. *Mathematical Geology*. 36 (7): 803-826.

[42]. Porwal, A., Carranza, E.J.M. and Hale, M. (2003). Knowledge-driven and data-driven fuzzy models for predictive mineral potential mapping. *Natural Resources Research*. 12 (1): 1-25.

[43]. Porwal, A., Carranza, E.J.M. and Hale, M. (2006). A hybrid fuzzy weights-of-evidence model for mineral potential mapping. *Natural Resources Research*. 15 (1): 1-14.

[44]. Gholami, R., Moradzadeh, A. and Yousefi, M. (2012). Assessing the performance of independent component analysis in remote sensing data processing. *Journal of the Indian Society of Remote Sensing*. 40 (4): 577-588.

[45]. Mandelbrot, B.B. (1983). *The Fractal Geometry of Nature*, W. H. Freeman, San Fransisco. 468 P.

[46]. Nazarpour, A. (2018). Application of C-A fractal model and exploratory data analysis (EDA) to

delineate geochemical anomalies in the: Takab 1:25,000 geochemical sheet, NW Iran. *Iranian Journal of Earth Sciences*. 10 (2): 173-180.

[47]. Afzal, P., Harati, H., Alghalandis, Y.F. and Yasrebi, A.B. (2013). Application of spectrum–area fractal model to identify of geochemical anomalies based on soil data in Kahang porphyry-type Cu deposit, Iran. *Chemie der Erde-Geochemistry*. 73 (4): 533-543.

[48]. Afzal, P., Khakzad, A., Moarefvand, P., Omran, N.R., Esfandiari, B. and Alghalandis, Y.F. (2010). Geochemical anomaly separation by multifractal modeling in Kahang (Gor Gor) porphyry system, Central Iran. *Journal of Geochemical Exploration*. 104 (1-2): 34-46.

[49]. Mihalasky, M.J. and Bonham-Carter, G.F. (2001). Lithodiversity and its spatial association with metallic mineral sites, Great Basin of Nevada. *Natural Resources Research*. 10 (3): 209-226.

یافتن پتانسیل‌های کانه‌زایی کرومیت انبانه‌ای با استفاده از شاخص ژئوشیمیایی و آنالیز فاکتوری مرحله‌ای در منطقه بلورد (جنوب شرقی ایران)

پیمان افضل^{۱*}، مهیار یوسفی^۲، میثاق میرزایی^۱، الهام قدیری صوفی^۳، سعید قاسم‌زاده^۴ و لی لی دانشور صابین^۵

۱- بخش مهندسی نفت و معدن، واحد تهران جنوب، دانشگاه آزاد اسلامی، ایران

۲- دانشکده فنی و مهندسی، دانشگاه ملایر، ایران

۳- گروه مهندسی معدن، دانشگاه کاشان، ایران

۴- دانشکده مهندسی معدن و متالورژی، دانشگاه صنعتی امیرکبیر، ایران

۵- گروه زمین‌شناسی، دانشگاه پیام نور، تهران، ایران

ارسال ۲۰۱۹/۲/۱۹، پذیرش ۲۰۱۹/۶/۹

* نویسنده مسئول مکاتبات: p_afzal@azad.ac.ir

چکیده:

هدف اصلی این پژوهش تعیین پتانسیل‌های کانه‌زایی کرومیت انبانه‌ای در منطقه بلورد (جنوب شرقی ایران) با استفاده از آنالیز فاکتوری مرحله‌ای و نیز شاخص ژئوشیمیایی مربوطه می‌باشد. به همین جهت در این مطالعه از داده‌های رسوب آبراهه‌ای و تراکم گسل‌ها استفاده شد. همچنین از عملگر فازی برای دو لایه ذکر شده استفاده شده است. همچنین از مدل‌سازی فرکتالی برای دسته‌بندی لایه‌های فازی شده و نیز نتیجه نهایی استفاده شده است. در ادامه از منحنی پیش‌بینی در برابر مساحت تحت پوشش کانی‌سازی‌ها و کانسارها برای صحت‌سنجی نتایج ترسیم و تحلیل شده است. بر این اساس ۸۲ درصد از کانه‌زایی‌های پیش‌بینی شده در ۱۸ درصد از مساحت منطقه مورد مطالعه قرار گرفته‌اند. پتانسیل‌های به دست آمده با مشخصات زمین‌شناسی کانسارهای کرومیت انبانه‌ای مورد مقایسه قرار گرفته و همپوشانی این مناطق با سنگ‌های اولترابازیک و آلتراسیون سرپانتینیتی نشانه‌های مهمی از صحت این پتانسیل‌ها می‌باشند.

کلمات کلیدی: شاخص ژئوشیمیایی مربوط به تیپ کانه‌زایی، آنالیز فاکتوری مرحله‌ای، وزن‌دهی ممتد، منطق فازی، کرومیت تیپ انبانه‌ای.
